COBEM 2021 26th International Congress of Mechanical Engineering
November 22-26, 2021, Virtual Congress, Brazil

COB-2021-1592
A STUDY ON IMAGE PRE-PROCESSING AND PIV PROCESSING TECHNIQUES FOR FLUID FLOWS

William Denner Pires Fonseca[a,1]
Rafael Franklin Lazaro de Cerqueira[b,2]
Erick de Moraes Franklin[a,3]
[a]School of Mechanical Engineering, University of Campinas
[b]Center for Petroleum Studies, University of Campinas
[1]fonsecawdp@gmail.com, [2]rafaelfc@unicamp.br, [3]franklin@fem.unicamp.br

Abstract. *Particle Image Velocimetry (PIV) is a non-intrusive and quantitative technique used for the visualization and measurement of deformation rates in fluid flows. The performance of the PIV technique is determined by the quality of the recorded images and treatment of the data obtained after the acquisition. The PIV technique heavily depends on the quality of the acquired images, i.e., homogeneous lighting, good contrast, low background noise, and suitable particle displacement. However, these conditions cannot always be achieved, and image pre-processing becomes an important tool for an accurate analysis of the problem. In the PIV pre-processing step, the aim is to enhance the correlation signal (displacement peak) and, therefore, produce higher quality vector fields based on contrast improvement, brightness correction, and noise removal. After the pre-processing step, the displacement vector is computed using a PIV correlation algorithm to obtain the velocity field in the next step. This work aims to evaluate and compare the performance of PIV image pre-processing and processing techniques. For this, two types of flows were used, Poiseuille flow and Rankine vortex, created from a PIV image generator and processed using the PIVlab toolbox, both coded in MATLAB. Three image pre-processing methods are analyzed: i) Contrast Limited Adaptive Histogram Equalization (CLAHE); ii) intensity high-pass and; iii) intensity capping. The accuracy of the DCC (Direct-Cross-Correlation) and DFT (Discrete Fourier Transform) algorithms are also evaluated and discussed.*

Keywords: *Particle Image Velocimetry, Pre-processing, Processing Techniques*

1. INTRODUCTION

In fluid mechanics, analytical approaches are not always able to solve complex problems due to the non-uniformity of geometries and boundary conditions. In fact, many of the practical engineering situations that involve fluid flows are physically and geometrically complex and hence demand the application of experimental approaches, such as techniques for flow visualization (Fox *et al.*, 2020).

Nowadays, the techniques for flow visualization are especially suitable for producing images that may be used to measure the fluid velocity, identify streamlines, and estimate turbulence related quantities. These techniques provide qualitative and quantitative data for the study of flows (Perissinotto *et al.*, 2021). In the last three decades, those that use solid seeding particles to estimate the velocity fields of fluid flows have stood out (Smits, 2012). This is, in fact, the basis for the operation of the PIV (Particle Image Velocimetry) method. PIV is a well-established optical measurement technique and many works on its fundamentals may be found in the literature, for example, Keane and Adrian (1990); Adrian (1991); Willert and Gharib (1991); Buchhave (1992); Adrian (1997, 2005); Adrian and Westerweel (2011); Raffel *et al.* (2018). The general principle is the addition of seeding particles to the fluid that move under the action of the flow structure of interest. Then, with an appropriate number of tracers, an adequate illumination setup, a camera and a synchronizing device, the flow field can be rigorously reconstructed with the help of image correlation algorithms.

The flow field is usually illuminated by a planar light source (usually a laser source) to highlight the particle locations in the region of interest. The light scattered by the tracer particles is captured by a high-resolution camera. Through the acquisition of two images (or frames), formed by two pulses of the laser plane in sequence (t_0 and $t_0 + \Delta t$), it is possible to obtain the particle displacement between two acquisitions through correlation methods. From the average particle displacement and the information of the period between the two pulses of illumination, it is possible to calculate the velocity field in a given region of the image.

Figure 1 presents the main components of a typical PIV system: a laser source, a digital camera, and an electronic circuit responsible for synchronizing each pulse emitted by the laser with each image captured by the camera. In addition, a set of mirrors and lenses are fixed in front of the laser cavity to convert the laser beam into a thin sheet that finally illuminates a plane region of the flow.

All the devices are connected to a computer that processes the images to calculate the fluid velocity vectors and other quantities dependent on their derivatives and integrals, such as gradient tensors, vorticity vectors, linear and angular deformations, and circulation integrals that reveal the presence of vortices. The procedure basically consists of dividing each pair of images into small regions, called interrogation windows, and then identifying the movement of the particles from differences in light intensity. The statistical concept of correlation is then used to compute the average displacement of a group of tracers. As a result, the algorithm provides a correlation map with a peak intensity for each pair of interrogation windows. This peak intensity corresponds to a velocity vector that represents an estimated measure of the local fluid velocity. The algorithm is then repeated for other interrogation windows and other pairs of flow images as well.

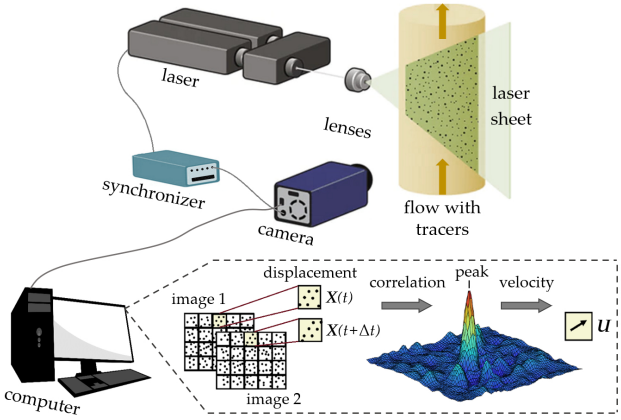

Figure 1: Schematic illustration of a conventional PIV system.
Extracted from Perissinotto *et al.* (2021).

The performance of the PIV technique is determined by the quality of the recorded images and the treatment of the data obtained after the acquisition (Raffel *et al.*, 2018). Image processing is facilitated if the quality of the original images is adequate, i.e., homogeneous lighting, good contrast, low background noise, and displacement of particles from a suitable tracer. However, when these conditions are not achieved, the optimization of parameters in the image acquisition procedure, as well as pre-processing and processing techniques, becomes an important tool for analyzing the problem.

Many works have been published on the optimization and errors quantification of experimental PIV parameters. Among those, the most relevant are noise in the recordings (Huang *et al.*, 1997), out-of-plane motion (Nobach and Bodenschatz, 2009), peak-locking due to small particle images (Westerweel, 1997; Christensen, 2004; Charonko and Vlachos, 2013) and velocity gradients (Meunier and Leweke, 2003; Westerweel, 2008). Also particle diameter, sub-pixel displacement and image density play a role on the measurement precision (Westerweel, 2000). All these errors can be mitigated or exacerbated depending on the choice of PIV operating parameters. This concurrence of parameters makes quantifying PIV uncertainty a non-trivial task.

The present work aims to evaluate and compare the performance of PIV image pre-processing and processing techniques. For this, two types of flows were used, Poiseuille flow and Rankine vortex, created from a PIV image generator and processed using the PIVlab toolbox (Thielicke and Stamhuis, 2014; Thielicke and Sonntag, 2021). Three image pre-processing methods were analyzed: i) Contrast Limited Adaptive Histogram Equalization (CLAHE); ii) intensity high-pass and; iii) intensity capping. The error related to each of these methods was quantified by the root mean square (RMS) of the mean velocity profile and evaluated in relation to particle diameter, particles density and background noise. The accuracy of the DCC (Direct Cross-Correlation) and DFT (Discrete Fourier Transform) algorithms are also evaluated and discussed.

2. IMAGE PRE-PROCESSING AND PIV PROCESSING TECHNIQUES

2.1 Image pre-processing

A common approach to improve the PIV measurement quality is the enhancement of images before real image correlation occur through pre-processing techniques (Thielicke and Stamhuis, 2014).

Contrast limited adaptive histogram equalization (CLAHE) is a relatively simple method for image enhancement. Several published works, such as (Pizer *et al.*, 1990; Zuiderveld, 1994; Pisano *et al.*, 1998; Reza, 2004), states that histogram equalization techniques can significantly improve the image quality in poor lightning condition. The standard procedure, in this case, is to remap the pixel intensity values of the image so that the resultant histogram approximates that of the uniform distribution. This procedure is based on the assumption that the image quality is uniform over all areas and one unique grayscale mapping provides a similar enhancement for all regions of the image. As a result, CLAHE

significantly improves the probability of detecting valid vectors in experimental images by 4.7 ± 3.2% (Thielicke and Stamhuis, 2014).

The high-pass filter is used to make an image appear sharper. This filter emphasizes the particle information in the image and suppresses any low-frequency information (including all low-frequency displacement information). High-pass filtering can also cause small, faint details to be greatly exaggerated. An over-processed image will look grainy and unnatural, and point sources will have dark around them. While high-pass filtering can often improve an image by sharpening detail, overdoing it can degrade the image quality significantly (Sciacchitano and Scarano, 2014).

A common source of error in the PIV technique is the presence of bright spots within the images. These bright spots are characterized by grayscale intensities much greater than the mean intensity of the image and are typically generated by intense scattering from seed particles. The displacement of bright spots can dominate the cross-correlation calculation within an interrogation window and may bias the resulting velocity vector. The intensity capping filter circumvents this problem. An upper limit of the grayscale intensity is selected, and this upper limit replaces all pixels that exceed the threshold. Therefore, unlike CLAHE, only a small amount of the pixel intensity information is adjusted, limiting the potential negative impact of image modifications. Intensity capping improves the probability of detecting valid vectors in experimental images by 5.2 ± 2.5% (Shavit *et al.*, 2007).

2.2 PIV processing techniques

After the pre-processing step, the PIV images are stored in pairs which have a specific time step between acquisitions. Transforming the recorded particle image pairs to a velocity vector field first involves dividing the images in the interrogation windows. The displacement vector is obtained from the PIV cross-correlation algorithm, which returns the average movement of small groups of particles (Raffel *et al.*, 2018). The cross-correlation algorithm is a statistical pattern matching technique that tries to find the particle pattern from interrogation window $A(t)$ back in interrogation window $B(t + dt)$. This statistical technique is implemented with the discrete cross-correlation function:

$$C(m,n) = \sum_{i}^{m} \sum_{j}^{n} I_1(i,j) \cdot I_2(i-m, j-n) \tag{1}$$

In Eq. (1), I_1 and I_2 denote the image intensity distribution of the first and second images, m and n the pixel offset between the two images. The location of the intensity peak in the resulting correlation matrix C gives the most probable displacement of the particles from I_1 to I_2 (Thielicke and Stamhuis, 2014). There are two common approaches to solve Eq.(1): one approach proposes to compute the correlation matrix in the spatial domain. This approach is also called Direct Cross-Correlation (DCC). Another approach, which is preferred due to this reduced computational cost, calculates the correlation matrix in the frequency domain (Discrete Fourier Transform, DFT) through the use of the Fast Fourier Transform (FFT).

The DCC computes the correlation matrix in the spatial domain. In a typical PIV acquisition, the images can be divided into hundreds of interrogation windows. Given the size of a square interrogation area A, a number of operations of the order of A^4 have to be computed (Keane and Adrian, 1992). Therefore, the DCC is an expensive computational technique. That is the main reason for introducing the fast Fourier transform into the cross-correlation process. The computational effort is reduced to the $O[A^2 \ln A]$, which means a considerable speed-up of the evaluation process of the cross-correlation function directly within a reasonable time-scale (Raffel *et al.*, 2018).

In the DFT approach, the local light intensity distributions contained in the interrogation windows are converted to the frequency domain to process the cross-correlation algorithm from the FFT. By multiplying the transform of the first image by the complex conjugate of the transform of the second one, the real and imaginary parts of the correlation map in the frequency domain are produced. The inverse FFT completes the operation and produces the correlation matrix C, given by Eq. (2):

$$C(m,n) = \Im^{-1}\{\Im[I_1(m,n)] \cdot \Im[I_2(m,n)]^*\} \tag{2}$$

where $\Im$ is the FFT operator of I_1 and I_2 and * represents their complex conjugate.

3. SYNTHETIC IMAGES GENERATOR AND IMAGES EVALUATION

Synthetic images are computer-generated PIV images that mimic true PIV images obtained in laboratory environments, while having zero-uncertainty ground truth (Rossi, 2019). Using synthetic images based on known flow data (from analytical solutions or numerically computed flow fields) makes it possible to know the exact solution, and true error, for specific cases. Synthetic images also allow for control of of PIV operating parameters, such as particle size, particle density and image background noise. In this work, the PIV images were generated from a synthetic-image-generator, coded in MATLAB, presented in Mendes *et al.* (2020).

The synthetically generated images for Poiseuille flow and Rankine vortex were treated from the PIVlab toolbox, coded in MATLAB (Thielicke and Stamhuis, 2014; Thielicke and Sonntag, 2021). Particles size, seeding density and noise level were varied in order to verify the error associated with each of the pre-processing and PIV processing methods. For this, the RMS error was computed from:

$$RMS = \sqrt{\frac{1}{N}\sum_{i=1}^{N}(U_m - U_s)^2} \tag{3}$$

where N is the number of samples, U_m is the mean velocity field post-processed from PIVlab toolbox for each method, and U_s is the velocity field extracted from the synthetic-image-generator.

Two hundred pairs of images were generated for each variation, where each had a size of 512 x 512 px. A constant displacement of 0.05 px was imposed. Motion estimation of the particles was given through multi-pass PIV, where the results of each pass are used to improve the estimation of the interrogation windows in the next pass. A three-pass PIV calculation that uses sequential interrogation windows sizes of 64, 32, and 16 px (step 50%) was used. To increase the accuracy of the results, the peak function is adjusted to determine particle displacement with sub-pixel precision. This estimate in PIVlab toolbox is adjusted by a Gaussian function.

4. RESULTS AND DISCUSSION

Figure 2 shows the RMS error as a function of the particles diameter for Poiseuille flow (Fig. 2a) and Rankine vortex flow (Fig. 2b). Particle sizes of 1.5, 3, 4.5 and 6 px were tested in this analysis, using a density of 6 particles per interrogation window and without any background noise. Three important consequences follow from this figure. First, the uncertainty decreases with increasing size particles no matter which pre-processing method is applied. According to Raffel *et al.* (2018), this is because the larger the size of particles considered for displacement estimation the better the statistical convergence. On the other hand, the increasing uncertainty with decreasing particles diameter is due to the fact that the image is not properly sampled. Small particle are typical if the observation distance is large and the magnification of the imaging system is small. In this case it might be an option to maximize the laser power and to slightly defocus the particle images in order to reach the optimal particles size range (Raffel *et al.*, 2018). Second, it is important to realize that for the two analyzed flows, the intensity capping pre-processing technique has higher associated errors than the other methods. CLAHE and intensity high-pass methods together with a image no processing approach have errors associated of the same order for the entire particles size range. Third, the associated error for the Poiseuille flow ranges from 0.55 to 0.62, while for the Rankine vortex it is around 0.28 to 0.34, thus being twice as small.

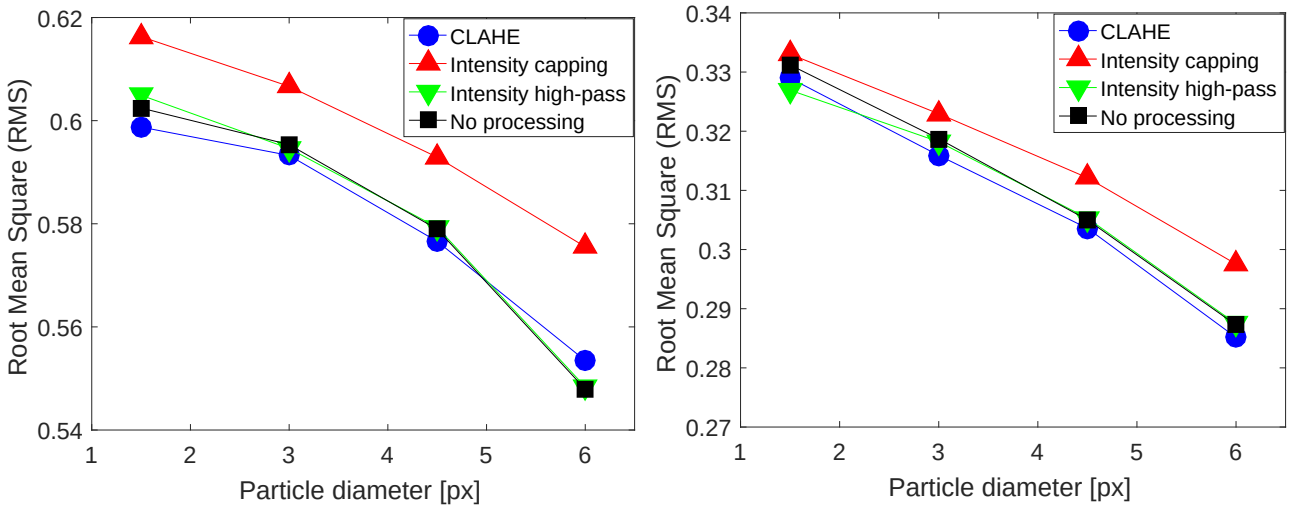

(a) Poiseuille flow

(b) Rankine vortex flow

Figure 2: RMS error as a function of particles diameter.

The results for the influence of particle density are shown in Fig. 3. Particle size 1.5 px in diameter with densities of 6, 12, 18 and 24 particles per interrogation window were used. Note that the error, both for the Poiseuille flow (Fig. 3a) and the Rankine vortex (Fig. 3b), decreases with the effective increase in the number of particles per interrogation window. Since the tracer particles are the information carriers within a PIV image, the displacement accuracy increases if the seeding densities is above a certain threshold.

Furthermore, it can be noted that for the Poiseuille flow, the error associated for the entire range of evaluated particles density are greater than for the Rankine vortex. Regarding the effectiveness of the methods, it is clear that the intensity high-pass and CLAHE approaches had the best performance.

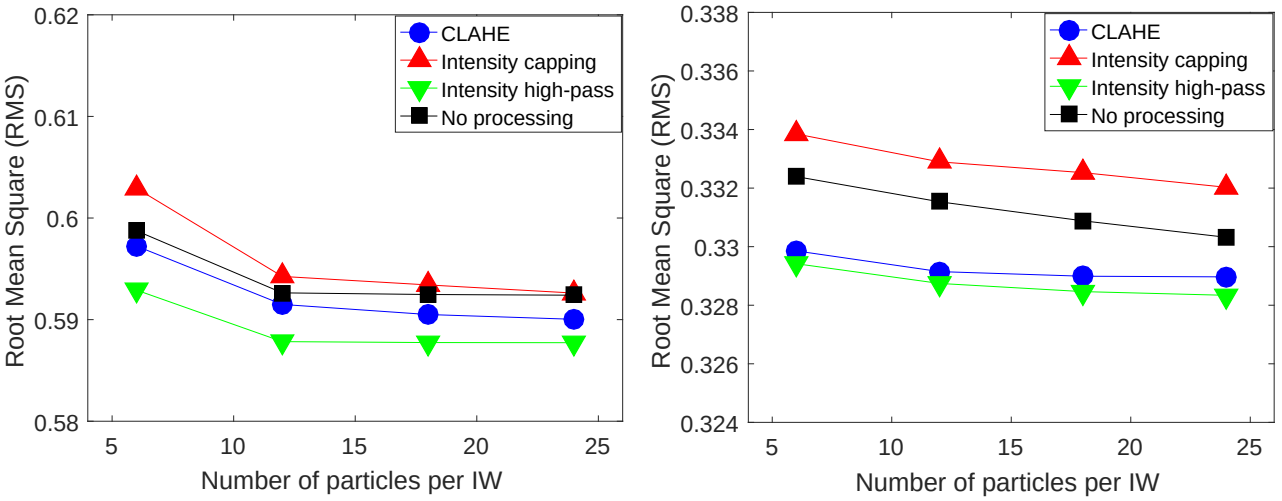

(a) Poiseuille flow (b) Rankine vortex flow

Figure 3: RMS error as a function of particle density.

Figure 4 presented the uncertainty due to background noise level for values of 0 (without background noise), 10, 20 and 30 dBW. Interrogation windows with density equal to 6 particles and particle sizes of 1.5 px in diameter were used. It can be seen that as the noise level increases, the associated error also increases. This is because background noise degrades the image representation of the tracer particles and hence the velocity field. For this analysis, the CLAHE and intensity capping methods had the best and worst performance, respectively. This is due to the fact that the images pre-processed by these approaches present highly different levels of background noise minimization, as shown in Fig. 5. Furthermore, it can be seen that for the Poiseuille flow the associated errors, as in the previous analyses, are higher than for the Rankine vortex flow. Note that for Poiseuille flow (Figs. 6a and 6b) the highest errors are concentrated in the regions close to the wall. This is a consequence of the low level of particle displacement close to this region, because the smaller the particle displacement, the greater the apparent error. Also note that for Rankine's vortex flow (Figs. 6c and 6d) the error associated between the core and the peripheral regions of the vortex remains approximately constant, with a difference of only 0.002 being computed between these regions for all analyzed pre-processing methods.

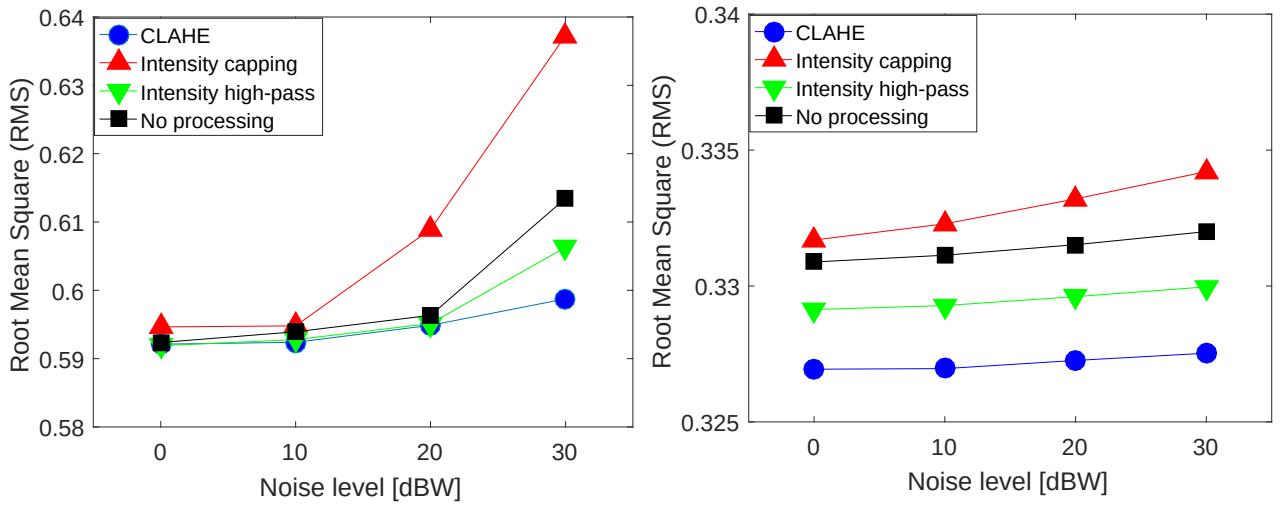

(a) Poiseuille flow (b) Rankine vortex flow

Figure 4: RMS error as a function of noise level.

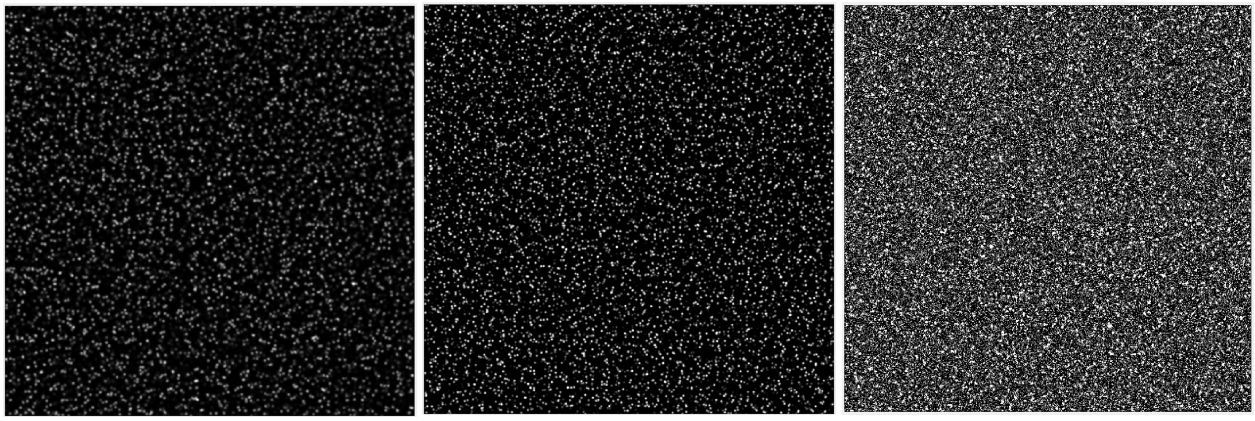

Figure 5: Illustration of the effect of different pre-processing method under the same noise level of 30 dBW.

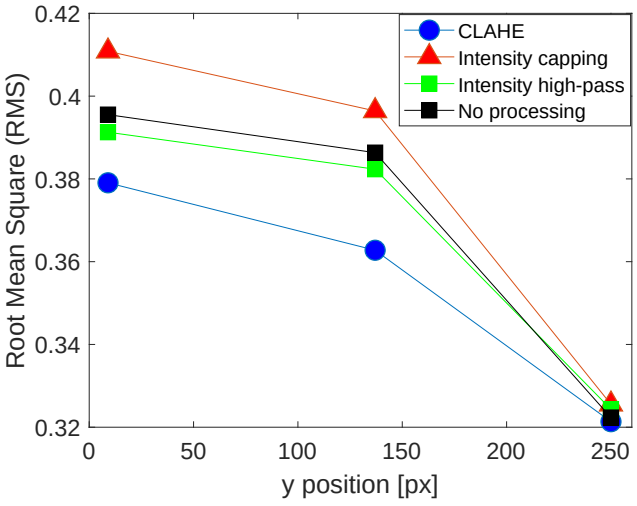

(a) Poiseuille flow no background noise

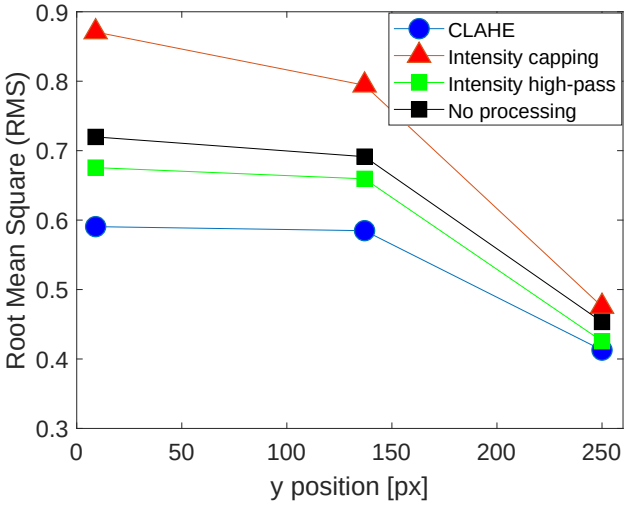

(b) Poiseuille flow with noise level of 30 dBW

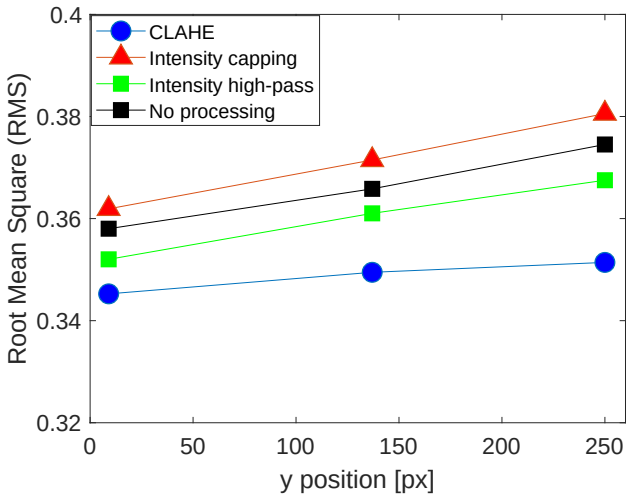

(c) Rankine vortex flow no background noise

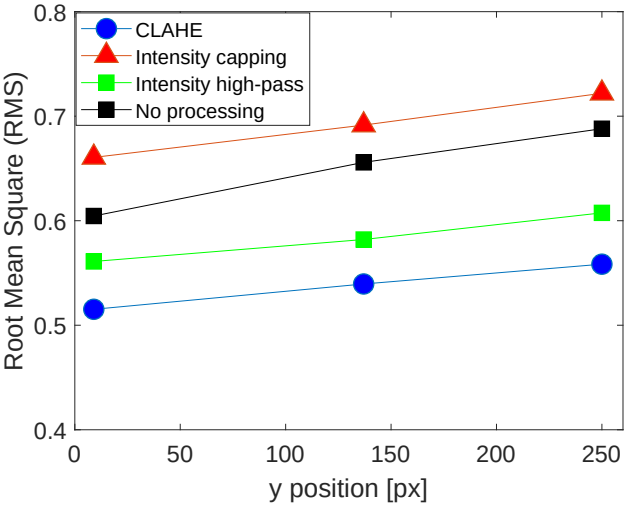

(d) Rankine vortex flow with noise level of 30 dBW

Figure 6: RMS error as a function of spatial position y.

In order to evaluate the accuracy of the PIV cross-correlation algorithms, tests for different noise levels were performed. Figure 7 presents the RMS error as a function of image background noise. From Fig. 7, it can be seen that the DFT image processing method has greater errors than those presented by the DCC method. According to Raffel *et al.* (2018), this is due to fact that the DFT method uses interrogation windows of same size, which induces loss of information in every particles displacement. On the other hand, in the analyzes performed it was found that the DFT algorithm is computationally more efficient than a direct computation of the correlation matrix using DCC approach, requiring around 30 seconds to process 200 pairs of images while the DCC method processes in 80 seconds.

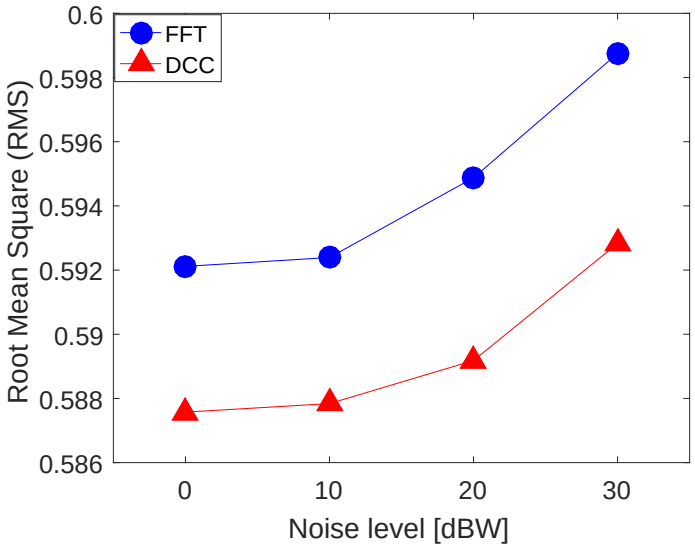

Figure 7: RMS error as a function of noise level; assessment of the accuracy of PIV processing techniques.

5. CONCLUSIONS

In this work, the performance of PIV image pre-processing and processing techniques was investigated. For that, synthetic PIV images of two idealized flows, Poiseuille flow and Rankine vortex flow, were generated through a computational routine and were processed in the PIVlab toolbox. PIV operating parameters were varied, such as particle diameter, particles density per interrogation window and background noise, and the error, deviation from the ground truth values, were evaluated. The results showed that for both analyzed flows, the error associated with each pre-processing method decreases both with increasing particle size and with increasing particle density, however, the RMS error increases with the image background noise. In addition, it was observed that the CLAHE pre-processing method obtained the best performance in all the performed analysis. The associated errors to Poiseuille flow were twice as large as those presented for the Rankine vortex flow, a consequence of the low displacement of particles in the regions close to the walls. Regarding the accuracy of PIV image processing methods, it was verified that the DCC approach had fewer errors compared to the DFT approach, however, the processing time presented in the DFT was approximately 2.5 times less than those processed by the DCC.

6. ACKNOWLEDGEMENTS

We gratefully acknowledge the support of EPIC – Energy Production Innovation Center, hosted by the University of Campinas (UNICAMP) and sponsored by Equinor Brazil and FAPESP - São Paulo Research Foundation (2017/15736–3). We also acknowledge the support of ANP (Brazil's National Oil, Natural Gas, and Biofuels Agency) through the R&D levy regulation. Acknowledgements are extended to the Center for Petroleum Studies (CEPETRO) and School of Mechanical Engineering (FEM) of the University of Campinas (UNICAMP).

7. REFERENCES

Adrian, R.J., 1991. "Particle-imaging techniques for experimental fluid mechanics". *Annual review of fluid mechanics*, Vol. 23, No. 1, pp. 261–304.

Adrian, R.J., 1997. "Dynamic ranges of velocity and spatial resolution of particle image velocimetry". *Measurement Science and Technology*, Vol. 8, No. 12, p. 1393.

Adrian, R.J., 2005. "Twenty years of particle image velocimetry". *Experiments in fluids*, Vol. 39, No. 2, pp. 159–169.

Adrian, R.J. and Westerweel, J., 2011. *Particle image velocimetry*. 30. Cambridge university press.

Buchhave, P., 1992. "Particle image velocimetry—status and trends". *Experimental Thermal and Fluid Science*, Vol. 5, No. 5, pp. 586–604.

Charonko, J.J. and Vlachos, P.P., 2013. "Estimation of uncertainty bounds for individual particle image velocimetry measurements from cross-correlation peak ratio". *Measurement Science and Technology*, Vol. 24, No. 6, p. 065301.

Christensen, K., 2004. "The influence of peak-locking errors on turbulence statistics computed from piv ensembles". *Experiments in fluids*, Vol. 36, No. 3, pp. 484–497.

Fox, R.W., McDonald, A.T. and Mitchell, J.W., 2020. *Introduction to fluid mechanics*. John Wiley & Sons, 10th edition.

Huang, H., Dabiri, D. and Gharib, M., 1997. "On errors of digital particle image velocimetry". *Measurement Science and Technology*, Vol. 8, No. 12, p. 1427.

Keane, R.D. and Adrian, R.J., 1990. "Optimization of particle image velocimeters. i. double pulsed systems". *Measurement science and technology*, Vol. 1, No. 11, p. 1202.

Keane, R.D. and Adrian, R.J., 1992. "Theory of cross-correlation analysis of piv images". *Applied scientific research*, Vol. 49, No. 3, pp. 191–215.

Mendes, L., Bernardino, A. and Ferreira, R.M., 2020. "piv-image-generator: An image generating software package for planar piv and optical flow benchmarking". *SoftwareX*, Vol. 12, p. 100537.

Meunier, P. and Leweke, T., 2003. "Analysis and treatment of errors due to high velocity gradients in particle image velocimetry". *Experiments in fluids*, Vol. 35, No. 5, pp. 408–421.

Nobach, H. and Bodenschatz, E., 2009. "Limitations of accuracy in piv due to individual variations of particle image intensities". *Experiments in fluids*, Vol. 47, No. 1, pp. 27–38.

Perissinotto, R.M., Verde, W.M., Biazussi, J.L., Bulgarelli, N.A.V., Fonseca, W.D.P., Castro, M.S., Franklin, E.M. and Bannwart, A.C., 2021. "Flow visualization in centrifugal pumps: A review of methods and experimental studies". *Journal of Petroleum Science and Engineering*, p. 108582.

Pisano, E.D., Zong, S., Hemminger, B.M., DeLuca, M., Johnston, R.E., Muller, K., Braeuning, M.P. and Pizer, S.M., 1998. "Contrast limited adaptive histogram equalization image processing to improve the detection of simulated spiculations in dense mammograms". *Journal of Digital imaging*, Vol. 11, No. 4, p. 193.

Pizer, S.M., Johnston, R.E., Ericksen, J.P., Yankaskas, B.C. and Muller, K.E., 1990. "Contrast-limited adaptive histogram equalization: speed and effectiveness". In *[1990] Proceedings of the First Conference on Visualization in Biomedical Computing*. IEEE Computer Society, pp. 337–338.

Raffel, M., Willert, C.E., Scarano, F., Kähler, C.J., Wereley, S.T. and Kompenhans, J., 2018. *Particle image velocimetry: a practical guide*. Springer.

Reza, A.M., 2004. "Realization of the contrast limited adaptive histogram equalization (clahe) for real-time image enhancement". *Journal of VLSI signal processing systems for signal, image and video technology*, Vol. 38, No. 1, pp. 35–44.

Rossi, M., 2019. "Synthetic image generator for defocusing and astigmatic piv/ptv". *Measurement Science and Technology*, Vol. 31, No. 1, p. 017003.

Sciacchitano, A. and Scarano, F., 2014. "Elimination of piv light reflections via a temporal high pass filter". *Measurement Science and Technology*, Vol. 25, No. 8, p. 084009.

Shavit, U., Lowe, R.J. and Steinbuck, J.V., 2007. "Intensity capping: a simple method to improve cross-correlation piv results". *Experiments in Fluids*, Vol. 42, No. 2, pp. 225–240.

Smits, A.J., 2012. *Flow visualization: techniques and examples*. World Scientific.

Thielicke, W. and Sonntag, R., 2021. "Particle image velocimetry for matlab: Accuracy and enhanced algorithms in pivlab". *Journal of Open Research Software*, Vol. 9, No. 1.

Thielicke, W. and Stamhuis, E., 2014. "Pivlab–towards user-friendly, affordable and accurate digital particle image velocimetry in matlab". *Journal of open research software*, Vol. 2, No. 1.

Westerweel, J., 2008. "On velocity gradients in piv interrogation". *Experiments in Fluids*, Vol. 44, No. 5, pp. 831–842.

Westerweel, J., 1997. "Fundamentals of digital particle image velocimetry". *Measurement science and technology*, Vol. 8, No. 12, p. 1379.

Westerweel, J., 2000. "Theoretical analysis of the measurement precision in particle image velocimetry". *Experiments in Fluids*, Vol. 29, No. 1, pp. S003–S012.

Willert, C.E. and Gharib, M., 1991. "Digital particle image velocimetry". *Experiments in fluids*, Vol. 10, No. 4, pp. 181–193.

Zuiderveld, K., 1994. "Contrast limited adaptive histogram equalization". *Graphics gems*, pp. 474–485.

8. RESPONSIBILITY NOTICE

The authors are solely responsible for the printed material included in this paper.